



Toward next-generation BNP/NT-proBNP biosensors: multiplexed detection, biofouling control, and digital health integration

Title	Toward next-generation BNP/NT-proBNP biosensors: multiplexed detection, biofouling control, and digital health integration
Author(s)	Varghese Rajendran, Jose;Elahi, Adnan;Scully, Patricia
Publication Date	2025-12-02
Publisher	Springer
Repository DOI	https://doi.org/10.1007/s10741-025-10573-4

1 Toward Next-Generation BNP/NT-proBNP Biosensors: 2 Multiplexed Detection, Biofouling Control, and Digital 3 Health Integration

4 Jose Varghese Rajendran^a, Adnan Elahi^{a,c,d}, Patricia Scully^{a,b}

5 ^aResearch Ireland Centre for Medical Devices (CÚRAM), University of Galway, Biomedical
6 Sciences Building, Newcastle Road, Galway, H91 W2TY, Ireland.

7 ^bPolymer Sensors and Devices Lab, School of Physics, University of Galway, Galway,
8 Ireland.

9
10 ^cTranslational Medical Device Lab, University of Galway, Galway, H91 TK33, Ireland.

11 ^dElectrical and Electronic Engineering, University of Galway, Galway, H91 TK33, Ireland.

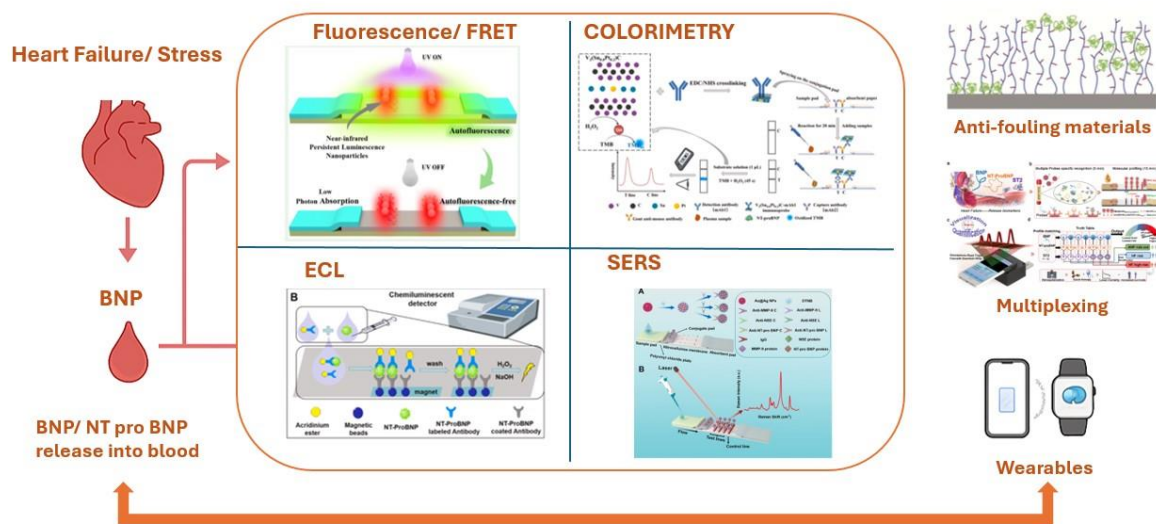
12 Corresponding author: Jose Varghese Rajendran; Email: josv3209@gmail.com ;
13 jose.rajendran@universityofgalway.ie

14 **Abstract**

15 In the past five years, rapid progress has been made in **biosensor platforms** for BNP and NT-
16 proBNP detection. Innovations span **fluorescence-based assays (FRET aptasensors,**
17 **quantum dots, NIR persistent luminescence probes), colorimetric nanozyme-enhanced**
18 **lateral flow assays, surface-enhanced Raman scattering (SERS) systems**
19 **and electrochemiluminescence immunoassays**. These strategies exploit advances in
20 nanomaterials, photonic engineering, and biointerface design to achieve femtogram-to-
21 picogram limits of detection, multiplex biomarker analysis, and smartphone-compatible
22 readouts. Parallel work on **biofouling mitigation** through zwitterionic coatings, hydrogel
23 nanocomposites, and MOF encapsulation can be adapted for further enhance sensor robustness
24 in complex biological fluids.

25 This review critically evaluates BNP/NT-proBNP detection technologies reported between
26 2020 and 2025, comparing analytical performance, material design, and translational potential.
27 We highlight gaps between laboratory performance and clinical implementation, discuss
28 harmonisation with established commercial assays, and outline future directions in multiplexed
29 panels, wearable monitoring, and digital health integration. By synthesizing recent advances,
30 this work provides a roadmap toward biosensors capable of transforming HF care through
31 earlier diagnosis, decentralised testing, and proactive disease management.

32 **Keywords:** BNP/NT-proBNP; Biosensors; Heart failure diagnostics; Point-of-care testing



33

34 1. Introduction

35 Heart failure (HF) remains a major global health challenge, affecting over 64 million people
 36 worldwide and contributing substantially to morbidity, mortality, and healthcare costs [1].
 37 Despite therapeutic advances, the clinical management of HF is hampered by delayed
 38 diagnosis, nonspecific symptoms, and frequent rehospitalizations. Accurate and timely
 39 biomarker measurement has become indispensable for diagnosis, prognosis, and monitoring of
 40 therapy in HF patients [1]. Among the available biomarkers, **B-type natriuretic peptide**
 41 **(BNP)** and its cleavage product **N-terminal proBNP (NT-proBNP)** are considered the gold
 42 standards, endorsed by both European and American guidelines for HF diagnosis and risk
 43 stratification [2].

44 BNP is synthesized as pre-proBNP in cardiomyocytes and processed into the biologically
 45 active BNP and the inactive NT-proBNP fragment, both released into circulation in response
 46 to ventricular stretch and pressure overload [3]. Elevated concentrations correlate strongly with
 47 HF severity and are predictive of hospitalization and mortality. However, BNP has a short
 48 plasma half-life and is subject to enzymatic degradation. It is also cleared through receptor-
 49 mediated internalization via natriuretic peptide receptors (NPR-A and NPR-C) and by renal
 50 filtration, contributing to reduced circulating concentrations[4]. In contrast NT-proBNP is
 51 more stable, making it the preferred analyte for routine diagnostics [5]. Both peptides rise
 52 proportionally with ventricular wall stress and are considered diagnostically equivalent in acute
 53 heart failure settings according to ESC guidelines [6]. BNP, however, demonstrates greater
 54 biological variability, whereas NT-proBNP provides more stable measurements during chronic
 55 follow-up[7][8]

56 The widespread clinical use of BNP and NT-proBNP is supported by robust evidence and
 57 international guidelines. The 2021 ESC and 2022 ACC/AHA/HFSA recommendations endorse
 58 either biomarker as a frontline diagnostic and prognostic tool [6]. While both assays perform
 59 comparably for HF diagnosis, pre-analytical and analytical variables including renal clearance,

60 assay-specific antibody pairs, and molecular heterogeneity can affect quantitative
61 agreement[7].

62 Currently, BNP and NT-proBNP are quantified using **central laboratory**
63 **immunoassays** (e.g., Roche Elecsys, Abbott Architect, Siemens Atellica) or **point-of-care**
64 **(POC) platforms** (e.g., Roche cobas h 232, Radiometer AQT90, LumiraDx) [9]. These
65 commercial assays deliver reliable performance and are deeply embedded in clinical
66 workflows. Nonetheless, they require specialized equipment, trained personnel, and in some
67 cases relatively long turnaround times. Furthermore, issues such as **assay bias across**
68 **platforms, susceptibility to biotin interference, and glycosylation-dependent epitope**
69 **masking** remain unresolved. These limitations highlight the urgent need for new detection
70 strategies that combine the sensitivity and specificity of laboratory assays with the speed,
71 portability, and affordability required for POC testing [10].

72 Assay bias across platforms often arises from variable recognition of glycosylated epitopes and
73 biotin interference. Recent studies demonstrated that BNP assays frequently detect
74 glycosylated proBNP forms, whereas NT-proBNP immunoassays mostly derived from
75 Roche's Elecsys design exhibit reduced inter-platform variability [11]. Moreover,
76 contemporary analyses have shown that glycosylation patterns significantly influence
77 immunoassay response and comparability across platforms [12].

78 Over the past five years, there has been rapid progress in **next generation biosensors** for
79 BNP/NT-proBNP, leveraging advances in nanomaterials, photonic structures, and biointerface
80 engineering. Techniques such as **fluorescence (FRET, QDs, NIR persistent luminescence),**
81 **colorimetric and nanozyme-enhanced LFIA, surface-enhanced Raman scattering (SERS)**
82 **and electrochemiluminescence (ECL) assays** have demonstrated femtogram-to-picogram
83 sensitivity, multiplexing capability, and compatibility with portable or smartphone-based
84 readers [13]. Parallel efforts in **biofouling mitigation, assay miniaturization, and digital**
85 **connectivity** are driving these platforms closer to clinical translation.

86 This review critically examines recent advances in BNP and NT-proBNP biosensors from 2020
87 to 2025, with emphasis on **optical detection strategies** and their integration into POC formats.
88 Several comprehensive reviews published before 2020 have thoroughly summarized early
89 developments in BNP/NT-proBNP detection technologies. For example, Maalouf and
90 Bailey[14] provided a foundational survey of assays and biosensors including implantable
91 platforms and Gachpazan et al. [15] classified detection strategies across electrochemical,
92 optical, microfluidic, and lateral-flow formats. Alawieh et al. [16] focused on the requirements
93 for point-of-care technologies and outlined key analytical metrics, while Sousa et al. [17]
94 synthesized broader cardiovascular biosensing trends. To maintain originality and emphasize
95 innovations relevant to clinical translation, this review deliberately concentrates on advances
96 reported from 2020 to 2025, a period marked by rapid strides in nanomaterial based
97 fluorescence, SERS, multiplexing, antifouling strategies, and integration with digital health
98 platforms. Previous reviews, including the 2022 article by Goryacheva et al., summarized early
99 optical-label detection strategies. However, since 2020, major advances have emerged in
100 multiplexed, glycosylation-independent, and antifouling-enhanced assays with integrated
101 digital readouts. This review specifically addresses the translational gap between analytical
102 innovation and clinical implementation, focusing on how nanomaterial-based and photonic
103 biosensors can bridge laboratory sensitivity with real world usability [2]. This review
104 emphasizes not only analytical sensitivity but also three emerging pillars, multiplexed

105 biomarker detection, antifouling surface engineering, and digital health integration that
106 collectively determine the clinical viability of BNP/NT-proBNP biosensors.

107 **2. Optical Label-Based Detection Techniques**

108 **2.1. Fluorescence-Based Immunoassays**

109 Fluorescence assays have emerged as one of the most sensitive and adaptable strategies for
110 BNP and NT-proBNP detection, enabling rapid and quantitative analysis with portable readers.
111 Compared with colorimetric immunoassays, which often plateau at nanogram-per-milliliter
112 sensitivity, fluorescence-based platforms routinely reach femtogram-per-milliliter levels while
113 supporting multiplexing and low sample volumes. Recent developments have largely been
114 driven by innovations in **energy transfer mechanisms (FRET), nanoparticle emitters**
115 **(quantum dots, persistent luminescence probes), and microchannel/magnetic**
116 **architectures** [18] [19] [20] [21].

117 **2.1.1 FRET-Based Fluorescence Sensors**

118 Förster resonance energy transfer (FRET) has been particularly effective for BNP/NT-proBNP
119 detection, exploiting donor–acceptor interactions that produce “turn-on” or “turn-off” signals
120 upon analyte binding. In these platforms, the **material choice for donor and quencher is**
121 **crucial** [18].

122 Graphene oxide (GO) is the most widely used quencher due to its broad absorption spectrum,
123 high quenching efficiency, and strong π – π interactions with nucleic acids. Tu et al. [19]
124 developed a GO–aptamer FRET sensor for BNP using a FAM-labeled aptamer probe,
125 achieving an **LOD of 45 fg/mL** with a dynamic range of **0.074–0.56 pg/mL**. Compared with
126 a Siemens chemiluminescent immunoassay, the FRET platform demonstrated superior ROC
127 specificity, highlighting the selectivity of aptamer recognition. Gong et al.[20] advanced this
128 approach for NT-proBNP detection in elderly heart failure patients, showing that their GO–
129 FRET aptasensor achieved **89.2% diagnostic accuracy and 89.5% specificity**, both higher
130 than the Siemens CLIA comparator (83.8% and 84.2%, respectively). This finding is
131 significant as it suggests aptamer-based recognition may mitigate false positives caused by
132 glycosylated epitopes or structurally related peptides.

133 Alternative donor–quencher systems have also been explored. Abraham et al.[21] reported
134 a **lanthanide-based FRET sensor**, using terbium–citrate complexes as long-lifetime donors
135 and MoS₂ nanosheets as quenchers. This system exploited the sharp emission and long
136 luminescence lifetime of terbium, combined with efficient spectral overlap with MoS₂,
137 producing a “turn-on” emission upon BNP binding. The assay achieved an **LOD of 3.87**
138 **pg/mL** with a range of **30–850 pg/mL**, validated in spiked serum samples. Although less
139 sensitive than GO–FRET systems, the lanthanide–MoS₂ design offered improved
140 photostability and robustness in biologically complex matrices.

141 Taken together, these studies show that FRET platforms consistently deliver **sub-picogram**
142 **detection limits**, outperforming conventional antibody-based fluorescence assays. The choice
143 of materials directly affects assay performance: GO provides unmatched sensitivity but suffers
144 from aptamer instability in whole blood, while lanthanide-based donors offer spectral
145 sharpness and stability at the cost of sensitivity. Importantly, clinical validation studies

146 demonstrate that FRET assays are not only analytically superior but can also outperform CLIA
147 platforms in specific patient populations.

148 **2.1.2 Nanoparticle- and Channel-Based Fluorescence Platforms**

149 Beyond FRET, nanoparticle emitters and novel assay architectures have broadened the scope
150 of fluorescence assays. Quantum-dot (QD) nanoprobes have been applied to multiplexed heart
151 failure diagnostics. A **triple-cascade quantum strip (TCQS)** combined QD nanobeads
152 functionalized with antibodies against BNP, NT-proBNP, and sST2, enabling simultaneous
153 quantification with a smartphone reader [22]. Reported LODs were **72–97 pg/mL for**
154 **BNP/NT-proBNP** and ~ 0.95 ng/mL for sST2, with $\sim 93\%$ clinical accuracy. The rationale for
155 using QDs lies in their high quantum yield and tunable emission, which allow simultaneous
156 multi-wavelength detection without cross-talk, a significant step toward syndromic POC
157 diagnostics.

158 To reduce autofluorescence interference, near-infrared persistent luminescence nanoparticles
159 (NIR-PLNPs) have been employed [23]. These probes emit in the NIR region and can be read
160 after excitation is switched off, eliminating autofluorescence from nitrocellulose and blood. An
161 NT-proBNP PLNP assay achieved an **LOD of 15 pg/mL**, high recovery (94–101%), and strong
162 agreement with Roche ECLI. While less sensitive than FRET sensors, PLNP strips are more
163 manufacturable and resilient in clinical matrices, making them suitable for routine field
164 applications.

165 Finally, **fluorescent magnetic lateral-flow channels** represent a pragmatic approach
166 emphasizing usability. By replacing membranes with microchannels and integrating
167 streptavidin magnetic beads, these assays create 3D capture zones that improve binding
168 efficiency. Coupled with fluorescent nanoparticles, this design achieved an **LOD of 43**
169 **pg/mL** using only **15 μ L of whole blood**, an order of magnitude less than commercial strip
170 assay. All reagents were pre-dried, supporting stability and field deployment [24].

171 Across these platforms, **material design drives both sensitivity and usability**. GO–aptamer
172 FRET systems remain unmatched in sensitivity (fg/mL) but require stabilization strategies for
173 real-world matrices. Lanthanide–MoS₂ FRET offers better robustness with modest sensitivity.
174 QD-based strips sacrifice some sensitivity but introduce **multiplexed HF panels** that align
175 with clinical workflows. NIR-PLNP probes strike a balance between sensitivity and robustness
176 by removing autofluorescence interference. Magnetic bead microchannels emphasize sample
177 efficiency and practical deployment, albeit with higher LODs.

178 Thus, fluorescence assays offer a **spectrum of trade-offs**: from research-grade ultra-sensitivity
179 (FRET) to clinically pragmatic multiplexing (QD), robustness (PLNP), and home-friendly
180 formats (magnetic LFC). The convergence of these strategies such as aptamer recognition with
181 NIR or QD probes integrated into microfluidic channels represents the most promising
182 trajectory for BNP/NT-proBNP biosensing over the next decade.

183 Fluorescence-based assays have begun transitioning from analytical proof of concept to
184 patient-sample validation. GO–FRET and NIR-PLNP assays have been evaluated in clinical
185 serum samples, showing $> 85\%$ agreement with Roche ECLIA reference methods and
186 excellent linearity across clinically relevant ranges. However, most demonstrations remain
187 single center studies with limited cohort sizes, and further multicenter validation will be
188 essential before regulatory translation.

189 **2.2 Matrix Effects and Sample Handling**

190 Most optical BNP/NT-proBNP assays are validated using serum or plasma, matrices that
191 require centrifugation and trained personnel. In non core laboratory settings, such pre-
192 analytical steps offset the advantages of rapid biosensing. Whole blood assays, such as the
193 magnetic channel, circumvent this need but face challenges including autofluorescence,
194 viscosity, and cellular scattering. Future POC biosensors should incorporate on-chip plasma
195 separation or whole-blood-compatible optics to achieve <15 min total turnaround time[25]
196 [15].

197 **3.2. Surface-Enhanced Raman Scattering (SERS)**

198 Surface-enhanced Raman scattering (SERS) has gained prominence in BNP/NT-proBNP
199 biosensing due to its capacity for **single-molecule sensitivity** and **molecular fingerprinting**.
200 By exploiting localized surface plasmon resonances of noble metal nanostructures, SERS
201 enables signal amplification several orders of magnitude beyond fluorescence or colorimetry.
202 Recent work has focused on integrating SERS with **microfluidic chips**, **lateral-flow assays**,
203 and **paper-fluidic devices**, reflecting a push toward portable and cost-effective point-of-care
204 formats [26] [27] [28] .

205 **Microfluidic chip-integrated SERS platforms** highlight the advantages of combining
206 confinement, flow control, and signal enhancement in a compact geometry. Zheng et al. [26]
207 reported an all-fiber microfluidic SERS immunosensor for BNP detection. They used amino-
208 functionalized metal-organic frameworks (MOFs) to anchor Au-HEPES nanoparticles and
209 toluidine blue dye as Raman reporters, with a sandwich immunoassay format. To further
210 improve sensitivity, a magnetic CoFe₂O₄-Au nanoparticle capture probe was introduced. This
211 dual-tag strategy achieved **pg/mL-level sensitivity** with low sample volumes and high
212 throughput, while the fiber coupling enabled portability. The MOF shell was chosen for its high
213 surface area and tunable porosity, allowing dense AuNP loading and stable Raman reporter
214 encapsulation, thereby increasing enhancement factors and reproducibility.

215 **SERS-based lateral-flow immunoassays (LFIA)** have been particularly successful in
216 pushing BNP/NT-proBNP diagnostics toward real-world deployment. Wang et al. [27]
217 developed a dual-mode LFIA using Au@Ag core-shell nanoparticles labeled with 5,5'-
218 dithiobis-(2-nitrobenzoic acid) (DTNB). The bimetallic design was selected to combine the
219 plasmonic strength of Au with the stability and tunable resonance of Ag, resulting in strong
220 SERS amplification. The strip simultaneously quantified **NT-proBNP, MMP-9, and NSE**,
221 biomarkers linked to stroke prognosis, with LODs as low as **0.12 pg/mL for NT-proBNP**.
222 Clinical serum analysis showed strong agreement with ELISA, and the SERS readout reduced
223 the subjectivity associated with visual LFIA interpretation. This study demonstrates the
224 translational potential of **multiplex SERS-LFIA strips** for emergency and bedside
225 diagnostics.

226 **Paper-fluidic SERS immunoassays** represent the most cost-sensitive approach, designed for
227 deployment in underserved settings. Chaturvedi et al.[28] introduced a cotton- and
228 nitrocellulose-based cartridge integrated with a BNP-specific aptamer, monoclonal antibody,
229 and gold nanoparticles functionalized with a malachite green isothiocyanate Raman reporter.
230 Using a handheld 638 nm Raman reader, the platform detected BNP in the clinically relevant
231 range of **0.3–1 ng/mL**, corresponding to NYHA Stage II–IV heart failure. The dual-mode
232 capability (SERS and RGB-based colorimetric readout) was particularly valuable, enabling

233 both low-cost visual screening and quantitative Raman confirmation. Material choices here
234 prioritized **affordability, stability, and compatibility with community health workers**,
235 rather than achieving femtogram-level sensitivity.

236 SERS-based assays illustrate how **nanomaterial and platform design dictate assay**
237 **performance**. MOF-based microfluidic SERS chips achieve very low LODs with high
238 reproducibility, but rely on sophisticated fabrication. Au@Ag SERS-LFIA strips
239 deliver **ultra-trace sensitivity and multiplexing** in a user-friendly POC strip format, albeit
240 requiring a Raman reader. Paper-fluidic SERS platforms trade some sensitivity
241 for **affordability and accessibility**, making them attractive for rural or resource-limited
242 healthcare. Collectively, these approaches demonstrate SERS as one of the most powerful
243 strategies for BNP/NT-proBNP detection, with each material and platform tailored toward a
244 different **translation pathway: laboratory-grade ultrasensitivity, hospital emergency**
245 **diagnostics, or community-level screening**.

246 SERS based LFIA platforms have shown promising translational potential, particularly in
247 emergency and stroke-related cohorts where NT-proBNP and co-biomarkers were quantified
248 with sub-pg/mL sensitivity. Reported correlations with conventional ELISA exceed 0.9,
249 confirming analytical credibility. Remaining challenges include reader miniaturization, assay
250 standardization, and cost reduction to enable deployment beyond tertiary hospitals.

251 **3.3. Colorimetric Assays**

252 Colorimetric immunoassays remain one of the most widely used formats for BNP/NT-proBNP
253 detection owing to their low cost, portability, and ease of naked-eye interpretation. Traditional
254 enzyme-linked immunosorbent assays (ELISA) provide reliable quantification but are
255 constrained by long assay times, high reagent consumption, and laboratory-only applicability.
256 For example, Quagliariello et al.[29] employed conventional colorimetric and enzymatic
257 assays to quantify NT-proBNP, BNP, H-FABP, and inflammatory mediators in
258 cardiomyocyte/lymphocyte co-culture models exposed to immune checkpoint inhibitors.
259 Although effective for biomarker profiling, such ELISA-type assays require several hours and
260 cannot be deployed as point-of-care tests (POCT), underscoring the limitations of traditional
261 colorimetric formats in contexts requiring rapid cardiac monitoring.

262 Recent progress have sought to overcome these constraints by enhancing lateral flow
263 immunoassay (LFIA) sensitivity through advanced labeling strategies. Wang et al.[30] reported
264 a dual-mode LFIA combining conventional colorimetric bands with surface-enhanced Raman
265 scattering (SERS) readout using Au/Ag core-shell nanotags. In this multiplex platform,
266 simultaneous detection of MMP-9, NSE, and NT-proBNP was achieved. While the visual
267 colorimetric bands offered rapid qualitative detection, the SERS channel pushed limits of
268 detection (LOD) into the sub-pg/mL regime (NT-proBNP LOD ~ 0.00012 ng/mL), far
269 surpassing traditional AuNP-LFIA. This design demonstrates how coupling colorimetric
270 readout with a more sensitive optical channel can provide both user-friendly screening and
271 high-resolution quantification. However, the dependence on a Raman spectrometer restricts its
272 immediate translation to decentralized POCT.

273 An alternative strategy exploits **nanozyme-mediated catalytic amplification** to improve the
274 intrinsic sensitivity of colorimetric LFIA. Tan et al.[31] developed a peroxidase-mimicking
275 nanozyme based on a Pt-doped MAX phase, $V_2(\text{Sn}_{0.8}\text{Pt}_{0.2})\text{C}$. Incorporated as immunoprobes,
276 these nanozymes generated amplified blue colorimetric signals upon TMB oxidation, yielding

277 an unprecedented LOD of 0.0016 ng/mL (1.6 pg/mL) for NT-proBNP. Notably, the assay
278 maintained a wide linear range (0.02–71.64 ng/mL), effectively spanning the clinically
279 reportable concentrations of NT-proBNP, and outperformed conventional AuNP-LFIA by over
280 three orders of magnitude. Unlike hybrid SERS-LFIA, this approach retained simple visual
281 detection without specialized instrumentation, making it attractive for practical POCT in heart
282 failure monitoring.

283 Taken together, these studies highlight a spectrum of colorimetric assay performance. Classical
284 ELISA provides high specificity but limited timeliness for POCT; conventional AuNP-LFIA
285 offers speed but insufficient sensitivity; nanozyme-enhanced LFIA substantially bridges this
286 gap by combining colorimetric simplicity with analytical sensitivity approaching advanced
287 optical assays; and hybrid colorimetric–SERS LFIA achieves ultra-sensitivity and multiplexing
288 at the cost of requiring Raman readers. Thus, the choice of platform should be guided by the
289 intended clinical context: **nanozyme LFIA for frequent NT-proBNP monitoring in heart**
290 **failure, multiplex SERS-LFIA for syndromic panels in stroke or acute care,**
291 **and traditional ELISA for laboratory mechanistic studies.**

292 Nanozyme enhanced colorimetric LFIA have progressed from laboratory testing to pilot
293 clinical evaluations, demonstrating diagnostic concordance above 90 % with standard
294 immunoassays while reducing turnaround to under 15 min. These platforms are particularly
295 attractive for decentralized or resource-limited settings, though long term stability and large-
296 scale field validation remain pending.

297 **3.4. Chemiluminescence-Based Assays**

298 Chemiluminescence immunoassays (CLIA) and electrochemiluminescence immunoassays
299 (ECLIA) have emerged as cornerstone methods for NT-proBNP quantification in both research
300 and routine diagnostics. Their advantages include high sensitivity, broad dynamic range, and
301 compatibility with automation. Recent studies have introduced novel chemistries, optimized
302 enzyme labels, and evaluated clinical performance across commercial platforms, highlighting
303 both methodological advances and challenges in standardization [32] [33] [34] [35].

304 Early work by Chen et al.[32] evaluated the **HISCL NT-proBNP chemiluminescence assay**,
305 which uses alkaline phosphatase-labelled antibodies and magnetic bead separation. The assay
306 demonstrated strong precision (total CV <6%), broad linearity (6.1–39,737 pg/mL), and
307 excellent agreement with the Roche Elecsys NT-proBNP platform ($r \approx 0.98$). Importantly, no
308 high-dose hook effect was observed up to >100,000 pg/mL, confirming robustness for samples
309 with extreme biomarker levels. These findings established HISCL as a viable alternative to
310 existing CLIA analyzers in clinical laboratories.

311 Building on probe chemistry, Li et al. [33] introduced a **functional acridinium ester (AE-2)**
312 **probe** with hydrophilic modifications that improve solubility, antibody coupling efficiency,
313 and chemiluminescence intensity. Compared to traditional AE-based labels, AE-2 exhibited
314 higher biocompatibility and stronger signal generation, enabling sensitive NT-proBNP
315 detection in real patient samples. This study underscores how molecular engineering of
316 luminescent tags can overcome limitations of older chemiluminescent probes (poor solubility,
317 weak antibody conjugation), potentially pushing CL assays closer to POCT deployment.

318 In parallel, Li et al. [36] explored enzyme optimization by developing a reagent based on **high-**
319 **activity *Cobetia marina* alkaline phosphatase (CmAP)** for magnetic particle-based CLEIA.

320 The recombinant enzyme displayed an exceptionally high specific activity (~13,133 U/mg) and
321 stability at room temperature for four months, achieving an assay sensitivity of 0.58 ng/L.
322 Compared to conventional ALP, CmAP significantly enhanced detection limits and stability,
323 demonstrating how enzyme engineering can directly improve clinical assay performance.

324 Commercial platforms have also undergone rigorous validation. Lau et al. [34] assessed
325 the **Abbott Architect NT-proBNP immuno-chemiluminometric assay** against Roche
326 ECLIA across nearly 500 clinical samples. The Abbott assay showed strong correlation with
327 Roche ($r = 0.999$) and linearity across 0.7 – 41,501 pg/mL, with minimal biotin interference
328 even at supraphysiological levels. These results confirmed its clinical reliability and
329 applicability of ESC age-adjusted diagnostic cut-offs. Similarly, Cho et al. [37]
330 compared **three assays—Siemens Atellica IM (direct CL), Abbott Alere (microparticle**
331 **CL), and Roche Elecsys proBNP II (ECLIA)**. All demonstrated acceptable concordance, but
332 Roche’s ECLIA showed slightly higher specificity and positive likelihood ratios, reinforcing
333 its position as the clinical benchmark.

334 Most recently, Feng et al. [35] evaluated the **Mindray NT-proBNP CLIA assay** in 2277
335 healthy individuals. The study established robust age- and sex-specific reference ranges,
336 showing progressive NT-proBNP increases with age and consistently higher levels in women.
337 The Mindray assay exhibited strong analytical performance ($CV < 3.2\%$, $LOD \sim 10$ ng/L) and
338 high diagnostic accuracy at clinically relevant cut-offs (sensitivity 96.6%, specificity 92.3% at
339 125 ng/L). These findings provide critical population-based reference data for improving
340 interpretation of CLIA results in Asian populations.

341 Taken together, these studies illustrate how **chemiluminescent assays balance innovation in**
342 **probe/enzyme design with clinical standardization**. Functional acridinium esters and
343 engineered ALP labels demonstrate the potential for higher sensitivity and robustness, while
344 evaluations of Abbott, Siemens, Roche, and Mindray systems underscore the importance of
345 cross-platform harmonization. Although all platforms reliably detect NT-proBNP in clinical
346 practice, subtle differences in specificity, bias, and demographic reference values highlight
347 the need for continued standardization to ensure universal interpretability of NT-proBNP
348 results across laboratories and patient populations.

349 Chemiluminescent and electrochemiluminescent assays already represent the clinical gold
350 standard, validated across thousands of samples and multiple populations. Ongoing
351 refinements such as glycosylation-independent antibodies and engineered enzyme labels aim
352 to harmonize results between manufacturers and enable partial migration of CLIA principles
353 to compact, point of care analyzers.

354 Collectively, fluorescence and SERS platforms offer unmatched analytical sensitivity, while
355 colorimetric nanozyme assays emphasize simplicity and low cost. Chemiluminescence
356 systems, though less portable, remain the benchmark for standardization and clinical trust.
357 The translational trajectory thus progresses from research-grade sensitivity to regulated,
358 deployable systems highlighting the need for hybrid designs that combine simplicity,
359 robustness, and connectivity.

360

361 Table I. Summary of major developments in BNP/NT-proBNP biosensors reported between 2020–2025.

Detection Technique	Materials/Platform	LOD / Linear Range	Sample Type	Strengths	Limitations	Key References (2020–2025)
Fluorescence (GO–FRET)	FAM-labeled aptamer + graphene oxide quencher	45 fg/mL; 0.074–0.56 pg/mL	Serum	Ultra-sensitive; aptamer specificity; low background	Aptamer instability in whole blood	[19] [20]
Fluorescence (Lanthanide–FRET)	Tb–citrate donor + MoS ₂ nanosheets	3.87 pg/mL; 30–850 pg/mL	Spiked serum	Long lifetime, sharp emission; good stability	Lower sensitivity vs GO-FRET	[21]
Fluorescence (Quantum-Dot Multiplex)	QD nanobeads targeting BNP, NT-proBNP, sST2	72–97 pg/mL (BNP/NT-proBNP); ~0.95 ng/mL (sST2)	Serum	Multiplexed HF panel; smartphone readout	Less sensitive; complex labeling	[22]
Fluorescence (NIR-PLNP)	Zn–Ga–Sn–O:Cr ³⁺ , Y ³⁺ persistent luminescence nanoparticles	15 pg/mL; 50–5000 pg/mL	Serum	Autofluorescence suppression; time-gated detection	More complex probe synthesis	[23]
Fluorescence (Magnetic LFIA)	Streptavidin-coated magnetic beads + fluorescent probes	43 pg/mL	Whole blood (15 µL)	Very low sample volume; dried reagent stability	Moderate sensitivity	[24]
SERS (Microfluidic chip)	MOF-AuNP SERS tags + CoFe ₂ O ₄ -Au magnetic probes	~pg/mL	Serum	High reproducibility; fiber integration	Fabrication complexity	[26]
SERS (Au@Ag LFIA)	Au@Ag core–shell NPs + DTNB Raman tag	0.12 pg/mL (NT-proBNP)	Serum (stroke cohort)	Ultra-sensitive; multiplex (MMP-9, NSE)	Needs Raman reader	[30]
SERS (Paper-fluidic)	Aptamer/antibody + AuNP + malachite green Raman reporter	0.3–1 ng/mL	Serum	Low-cost; handheld Raman or visual readout	Lower sensitivity vs lab assays	[28]
Chemiluminescence (HISCL CLIA)	Alkaline phosphatase-labeled antibody; magnetic beads	6.1–39,737 pg/mL	Serum	Broad linearity; no hook effect; robust	Requires analyzer	[32]
Chemiluminescence (Abbott Architect)	Acridinium ester probes; microparticle CLIA	0.7–41,501 pg/mL	Serum	High correlation with Roche; low biotin interference	Platform dependent bias	[33]

Chemiluminescence (Mindray CLIA)	Enzyme-based chemiluminescent immunoassay	LOD ~10 ng/L; CV <3.2%	Serum (n=2277 healthy)	Age/sex reference ranges established	Needs benchtop analyzer	[35]
Fiber-optic immunosensor	Antibody-functionalized fiber tip with fluorescence/ECL readout	Low pg/mL range	Serum/plasma	High sensitivity; compact photonic design	Needs robust antifouling; early stage	[25]

362

364 **4. Biofouling Mitigation Strategies**

365 Biofouling, the non-specific adsorption of proteins, lipids, and cellular components from
366 complex biological fluids, is a pervasive challenge that affects nearly all biosensors designed
367 for clinical use. When sensors are exposed to matrices such as serum, plasma, or whole blood,
368 nonspecific adsorption can mask specific recognition events, elevate background signals, and
369 compromise reproducibility. Although this review centers on BNP and NT-proBNP detection,
370 the problem of biofouling is not unique to these biomarkers. Instead, it represents a fundamental
371 barrier to the translation of biosensors for any protein target into reliable point-of-care or
372 clinical diagnostic tools. [38] [39] [40].

373 **4.1 Zwitterionic Polymers and Advanced Brushes**

374 PEGylation has long been a go-to for anti-fouling, but emerging materials outperform
375 it. **Zwitterionic polymers** such as sulfobetaines and carboxybetaines resist protein adhesion
376 by forming a dense hydration shell and demonstrating remarkable stability under oxidative
377 stress. For instance, Wen et al. [38] summarize how zwitterionic polymer brushes achieve
378 ultra-low protein adsorption, making them highly promising for biosensor
379 interfaces. Similarly, Saxena et al. show that polymer-coated electrodes reduce protein
380 adsorption by around 67% compared to bare gold, demonstrating strong anti-fouling potential
381 for electrochemical biosensors [39].

382 Computational modeling studies further inform design: Regev et al. highlight the importance
383 of polymer chain density and pore architecture, showing that over-dense surfaces can repel
384 proteins more effectively—critical insight for fine-tuning sensor coatings [41]. Zwitterionic
385 polymers are particularly suited for electrochemical and fiber optic biosensors, where their
386 dense hydration layers and charge neutrality effectively repel proteins and cells from probe
387 surfaces, preserving optical transparency and signal fidelity.

388 **4.2 Zwitterionic Peptide Hydrogels**

389 Emerging materials that combine zwitterionic chemistry with hydrogel structure offer dual
390 benefits of hydration and antifouling. Du et al. reported a self-assembled, cysteine-terminal
391 zwitterionic peptide hydrogel immobilized on PEDOT/AuNP-modified electrodes, which not
392 only resisted nonspecific adsorption but also preserved biosensing sensitivity (limit of detection
393 ≈ 5.6 pg/mL) for prostate-specific antigen assays—suggesting such hydrogels could be adapted
394 to NT-proBNP sensors [40].

395 **4.3 Hydrogels and Nanocomposite Coatings**

396 Hydrogels, especially when integrated with conductive or porous nanocomposites, can provide
397 a hydrated, anti-adsorption matrix while enhancing signal transfer. Völlmecke et al. reviewed
398 hydrogel sensors noting their tunable chemistry, structural support, and sensitivity but also
399 point out fouling resistance as a key advantage [42]. More recently, Cui classified hydrogels
400 (nucleic-acid, synthetic polymer, natural polymer, carbon-based), emphasizing their roles in
401 building antifouling interfaces for photoelectrochemical sensors—a likely useful analogy for
402 optical BNP platforms[43]. Hydrogels are widely applied in optical and photoelectrochemical

403 sensors to form hydrated matrices that physically limit nonspecific adsorption while
404 maintaining high analyte diffusivity toward the recognition layer.

405 **4.4 MOF-Based Anti-Fouling Designs**

406 Metal–organic frameworks (MOFs) are gaining traction in SERS and optical biosensing, both
407 for embedding signal reporters and providing a protective matrix. Jiang et al. describe
408 antifouling MOF-based interfaces in electrochemical immunosensors that resist nonspecific
409 adsorption, suggesting MOFs could serve dual roles in SERS-LFIA or fiber-optic BNP
410 detection systems [34]. Similarly, Gu et al. review how MOF-based SERS substrates deliver
411 better stability and reproducibility—important for maintaining low fouling over repeated use
412 [44]. Metal organic frameworks (MOFs) serve dual functions in SERS and microfluidic
413 biosensors by encapsulating Raman reporters within porous cages and simultaneously
414 shielding active sites from biofouling.

415 Antifouling materials are critical enablers for translating BNP/NT-proBNP biosensors from
416 controlled laboratory environments to complex biological matrices such as whole blood and
417 interstitial fluid. Effective surface chemistries directly determine assay reproducibility,
418 stability, and compatibility with patient samples. Integrating zwitterionic polymers, hydrogels,
419 and MOF based coatings into next-generation sensor architectures will be essential to bridge
420 the gap between analytical sensitivity and reliable point of care performance.

421 **5. Commercial NT-proBNP Detection Technologies**

422 While novel biosensors show promise for point-of-care testing, **commercially available**
423 **immunoassays** for BNP and NT-proBNP remain the gold standard in both hospital
424 laboratories and decentralized care. These assays are primarily based on **immuno-**
425 **chemiluminescence, electrochemiluminescence (ECL), fluorescence immunoassay (FIA),**
426 **or lateral-flow immunoassay (LFIA)** technologies, and their performance sets the benchmark
427 against which emerging optical biosensors must be judged.

428

429 Table 2. Comparative summary of commercial BNP/NT-proBNP assays

430 Table 2 summarizes the main commercial BNP and NT-proBNP immunoassay systems currently used in clinical practice, highlighting their
 431 analytical performance, turnaround time, and suitability for various clinical settings.
 432

Manufacturer	Platform	Matrix	LOD (pg/mL)	Linear Range (pg/mL)	TAT (min)	Correlation (r)	Clinical Use	Ref
Roche Elecsys proBNP II	ECLIA (central lab)	Serum/Plasma	~5	5–35,000	18 (9 STAT)	≥0.98	Central lab gold standard	[45]
Abbott Architect NT-proBNP	CLIA (central lab)	Serum/Plasma	~10	0.7–41,500	~20	0.999	Routine hospital labs	[46]
Siemens Atellica IM (BNP/NT-proBNP)	Direct CL (central lab)	Plasma (EDTA/heparin)	~8	10–30,000	16–60	0.97	Hospital labs	[47]
Radiometer AQT90 FLEX (NT-proBNP/BNP)	Fluorescence immunoassay (POC)	Whole blood/Plasma	~15	20–15,000	11–21 (<11 NT-proBNP)	0.94	Emergency department	[48]
LumiraDx NT-proBNP	Microfluidic FIA (POC)	Capillary/Whole blood	~8–10	10–10,000	~12	0.95	Primary care / ED POC	[49]

433 *Notes for Siemens: documented measuring interval shown here is for **Atellica IM BNP** assay method sheet (plasma EDTA). NT-proBNP ranges and LODs vary by site and
 434 configuration; comparative r values are from a 3-assay study (Roche vs Abbott vs Siemens).

435

436 5.1 Central Laboratory Platforms

437 The most widely adopted analyzers are the **Roche Elecsys proBNP II (ECLIA)**, **Abbott**
438 **Architect NT-proBNP (chemiluminometric immunoassay)**, and **Siemens Atellica IM BNP**
439 **(direct chemiluminescence)** [45][46] [47]. Roche Elecsys remains the reference method in
440 most clinical studies, offering a linear range from ~5 to >35,000 pg/mL, LOD ~5 pg/mL, and
441 strong reproducibility (CV <5%). Cross-platform comparison studies between Roche, Abbott,
442 and Siemens consistently show high correlation ($r > 0.95$), although **biases of up to 20%** have
443 been reported at clinically relevant cut-offs.

444 Although current commercial assays achieve adequate sensitivity for HF diagnosis, enhancing
445 sensitivity could enable discrimination of specific BNP molecular forms. For instance, BNP
446 constitutes less than 5 % of total BNP signal in most assays. BNP-specific assays recently
447 developed demonstrated subtype selectivity but required higher analytical sensitivity to achieve
448 clinical utility [9]. Importantly, recent studies emphasize **glycosylation-dependent epitope**
449 **recognition** in conventional NT-proBNP assays, which may lead to underestimation in heavily
450 glycosylated patient samples. This has prompted interest in **glycosylation-independent total**
451 **NT-proBNP assays** now in early commercial development. Conventional NT-proBNP assays
452 recognize glycosylation-sensitive epitopes, occasionally underestimating concentrations in
453 highly glycosylated patient samples. Recently, glycosylation-independent antibody pairs have
454 been developed, targeting peptide backbones and offering improved cross-platform agreement.
455 Such assays may redefine diagnostic thresholds and are poised to become a new reference
456 standard in HF biomarker testing[7] .

457 Recent studies have reported glycosylation independent NT-proBNP assays that target peptide
458 backbones unaffected by O-glycan masking, improving cross-platform comparability [50].
459 Nonetheless, both BNP and NT-proBNP assays perform reliably in clinical use, and enhanced
460 specificity for molecular subtypes does not necessarily equate to improved diagnostic
461 performance.

462 5.2 Point-of-Care (POC) Systems

463 For emergency and primary care settings, POC BNP/NT-proBNP assays provide results in
464 10–20 minutes, enabling rapid triage of acute dyspnea. Commonly used systems include:

- 465 • **Roche cobas h 232** (BNP) – a handheld device measuring BNP in whole blood or
466 plasma (TAT ~12 min). It is widely used in European outpatient and GP clinics [51].
- 467 • **Radiometer AQT90 FLEX** (BNP and NT-proBNP) – benchtop immunoassay
468 analyzer delivering results in 12–15 min with correlation to central lab methods [48].
- 469 • **Siemens Stratus CS** – older generation device, gradually phased out but historically
470 important [52].
- 471 • **LumiraDx NT-proBNP Test** – a microfluidic FIA platform validated in ED cohorts
472 (2022–2024) showing strong agreement with Roche Cobas laboratory assays ($r > 0.95$)
473 and suitable for rule-in/rule-out cut-offs [49].

474 Recent clinical evaluations confirm that these POC systems offer **acceptable accuracy**
475 **compared to central lab assays**, although minor biases persist, particularly at low
476 concentration ranges relevant to early heart failure detection.

477 Commercial assays occupy different niches in the diagnostic pathway:

- 478 • **Central lab ECLIA/CLIA systems** (Roche, Abbott, Siemens) provide the most
479 reproducible results with broad dynamic ranges, but require trained personnel and
480 batch operation.
- 481 • **POC analyzers** (Roche h 232, AQT90 FLEX, LumiraDx) provide near-patient
482 answers within 15 minutes, essential for ED triage and GP clinics, but remain costlier
483 per test and slightly less precise at low levels.
- 484 • **Emerging glycosylation-independent assays** may represent the next paradigm shift,
485 potentially redefining reference values and “true” NT-proBNP concentrations.

486 In summary, **commercial BNP/NT-proBNP assays remain the gold standard**, offering
487 clinically validated accuracy and workflow integration. Novel optical biosensors must
488 demonstrate not only **ultra-low LODs** in buffer but also **equivalence to these established**
489 **commercial systems** across the full clinical range if they are to be translated into practice.

490 **6. Future Directions and Clinical Translation**

491 Despite rapid progress in BNP and NT-proBNP biosensor development, clinical adoption of
492 next-generation devices remains limited. Most prototypes demonstrate excellent analytical
493 sensitivity in buffered conditions, yet translation into patient care demands a broader
494 framework that integrates analytical robustness, clinical validation, manufacturability,
495 regulatory compliance, and health-system impact.

496 Many optical biosensors particularly FRET, SERS, and fiber-optic systems report
497 femtogram-to-picogram detection limits, far below the concentrations typically used in
498 clinical decision making (100–300 pg/mL). While such sensitivity is impressive, reliability
499 across the entire diagnostic window is far more critical. Future work should emphasize
500 linearity, reproducibility, and inter-assay comparability rather than focusing solely on ever-
501 lower LODs.

502 As highlighted across fluorescence, SERS, and fiber-optic platforms, **biofouling** remains a
503 major translational barrier. Antifouling strategies such as zwitterionic polymer brushes,
504 hydrogel nanocomposites, and MOF encapsulation show promise, but require systematic
505 validation in whole blood and plasma. Incorporating pre-analytical separation methods, such
506 as magnetic bead capture or microfluidic plasma extraction, could further improve assay
507 robustness under real-world conditions.

508 Heart failure management is increasingly shifting toward **multi-marker strategies** that
509 combine BNP/NT-proBNP with complementary biomarkers such as ST2, Galectin-3, and
510 high-sensitivity troponin. Recent advances in quantum-dot strips, SERS-LFIA, and magnetic
511 channel assays demonstrate that multiplex detection is feasible in compact formats. Such
512 platforms may enable syndromic biomarker panels capable of distinguishing acute dyspnea
513 etiologies and improving prognostic accuracy in a single test.

514 A parallel driver for translation is the integration of biosensors into **digital health**
515 **ecosystems**. Smartphone-based readers, cloud connectivity, and algorithmic risk scoring can
516 enable home based monitoring, particularly valuable in rural or resource-limited settings.
517 Persistent luminescence probes and aptamer based assays are well suited to this integration

518 due to their compact optics and wash-free workflows. In the longer term, minimally invasive
519 or wearable platforms such as microneedle patches and implantable fiber sensors could
520 enable continuous monitoring, shifting HF care from reactive to preventive.

521 For meaningful impact, future devices must also align with **regulatory and economic**
522 **frameworks**. Commercial assays such as Roche Elecsys and Abbott Architect set the
523 benchmark with multicenter validation and standardized cut-offs. Novel biosensors must
524 demonstrate method agreement with these systems while addressing population-specific
525 reference ranges. Early engagement with regulatory bodies and adherence to ISO 13485 and
526 IVDR/FDA requirements will accelerate adoption. Equally, translation requires proving cost-
527 effectiveness—reducing hospitalizations, enabling earlier interventions, and lowering overall
528 healthcare costs.

529 Precision requirements vary with clinical context. In acute triage, speed and high negative
530 predictive value are paramount, whereas in chronic follow-up, analytical reproducibility and
531 longitudinal comparability dominate. Next-generation BNP/NT-proBNP biosensors should
532 therefore be designed for dual-mode operation, rapid qualitative rule-out in emergencies and
533 precise quantitative trending for long-term monitoring.

534 **7. Conclusion**

535 BNP and NT-proBNP remain the most widely adopted biomarkers for the diagnosis, prognosis,
536 and monitoring of heart failure. While commercial chemiluminescent and
537 electrochemiluminescent assays continue to serve as clinical gold standards, they are
538 constrained by the need for centralized laboratories, trained personnel, and high infrastructure
539 costs. Over the past five years, advances in biosensing technologies have demonstrated
540 remarkable potential to address these limitations. Platforms based on **fluorescence (including**
541 **FRET, quantum dots, and persistent luminescence probes), colorimetry enhanced by**
542 **nanozymes, surface-enhanced Raman scattering (SERS), electrochemiluminescence, and**
543 **fiber-optic immunoassays** have achieved detection limits in the femtogram-to-picogram
544 range, multiplexing capability, and compatibility with smartphone-based or portable readers.
545 These innovations demonstrate the feasibility of rapid, low-cost, and highly sensitive assays
546 suitable for decentralized care.

547
548 However, translating these technologies from bench to bedside requires overcoming persistent
549 challenges. **Biofouling, matrix effects, and assay variability** remain major barriers to
550 reproducibility in complex biological samples. Promising mitigation strategies—such as
551 zwitterionic polymer brushes, hydrogel nanocomposites, and MOF encapsulation—have
552 shown efficacy, but require broader validation across clinical cohorts. Moreover, for true
553 impact, novel biosensors must demonstrate not only superior analytical sensitivity but
554 also **equivalence to commercial assays across clinically relevant ranges**, as well as
555 scalability, cost-effectiveness, and compliance with regulatory standards.

556
557 Looking forward, the most transformative direction lies in **multiplexed, digitally integrated,**
558 **and wearable biosensing platforms**. By combining BNP/NT-proBNP with complementary
559 biomarkers such as ST2, Galectin-3, and high-sensitivity troponin, and linking readouts to
560 cloud-based clinical decision systems, future devices may shift heart failure care from reactive
561 crisis management to proactive, personalized monitoring. With continued progress in materials
562 science, biointerface engineering, and digital health integration, next-generation BNP/NT-

563 proBNP biosensors are poised to move beyond laboratory prototypes and become **clinically**
564 **transformative tools for early diagnosis and long-term management of heart failure.**
565

566

567 **Contributions**

568 J.V.R. conceptualized the review, conducted the literature search, and drafted the manuscript.
569 A.E. reviewed the manuscript and provided guidance on translational aspects. P.S. provided
570 critical revisions and additional guidance on translational aspects. All authors reviewed and
571 approved the final manuscript.

572

573 **Funding**

574 This publication has emanated from research conducted with the financial support of EU
575 MSCA co-fund GA No 101081457 and Research Ireland grant number 13/RC/2073_P2.

576

577

578 **Reference**

579

580 [1] N. R. Jones, F. R. Hobbs, and C. J. Taylor, “Prognosis following a diagnosis of heart
581 failure and the role of primary care: a review of the literature,” *BJGP Open*, vol. 1, no.
582 3, p. bjgpopen17X101013, Oct. 2017, doi: 10.3399/bjgpopen17X101013.

583 [2] O. A. Goryacheva *et al.*, “Heart failure biomarkers BNP and NT-proBNP detection
584 using optical labels,” *TrAC Trends in Analytical Chemistry*, vol. 146, p. 116477, Jan.
585 2022, doi: 10.1016/j.trac.2021.116477.

586 [3] M. Weber, “Role of B-type natriuretic peptide (BNP) and NT-proBNP in clinical
587 routine,” *Heart*, vol. 92, no. 6, pp. 843–849, Oct. 2005, doi: 10.1136/hrt.2005.071233.

588 [4] C. Santos-Araújo, A. Leite-Moreira, and M. Pestana, “Clinical value of natriuretic
589 peptides in chronic kidney disease,” *Nefrología*, vol. 35, no. 3, pp. 227–233, May
590 2015, doi: 10.1016/j.nefro.2015.03.002.

591 [5] D. Moertl *et al.*, “Comparison of Midregional Pro-Atrial and B-Type Natriuretic
592 Peptides in Chronic Heart Failure,” *J Am Coll Cardiol*, vol. 53, no. 19, pp. 1783–1790,
593 May 2009, doi: 10.1016/j.jacc.2009.01.057.

594 [6] T. A. McDonagh *et al.*, “2021 ESC Guidelines for the diagnosis and treatment of acute
595 and chronic heart failure,” *Eur J Heart Fail*, vol. 24, no. 1, pp. 4–131, Jan. 2022, doi:
596 10.1002/ejhf.2333.

597 [7] T. Nishikimi *et al.*, “The effect of glycosylation on plasma N-terminal proBNP-76
598 levels in patients with heart or renal failure,” *Heart*, vol. 98, no. 2, pp. 152–161, Jan.
599 2012, doi: 10.1136/heartjnl-2011-300102.

600 [8] G. C. M. Linssen, T. Jaarsma, H. L. Hillege, A. A. Voors, and D. J. van Veldhuisen,
601 “A comparison of the prognostic value of BNP versus NT-proBNP after
602 hospitalisation for heart failure,” *Netherlands Heart Journal*, vol. 26, no. 10, pp. 486–
603 492, Oct. 2018, doi: 10.1007/s12471-018-1145-x.

604 [9] H. Alawieh, T. El Chemaly, S. Alam, and M. Khraiche, “Towards Point-of-Care Heart
605 Failure Diagnostic Platforms: BNP and NT-proBNP Biosensors,” *Sensors*, vol. 19, no.
606 22, p. 5003, Nov. 2019, doi: 10.3390/s19225003.

607 [10] A. A. Yousif *et al.*, “An Overview of Biotin Interference Impact on Immunoassays,”
608 *Cyprus Journal of Medical Sciences*, vol. 10, no. 3, pp. 162–168, Jun. 2025, doi:
609 10.4274/cjms.2025.2024-71.

610 [11] A. G. Semenov and A. G. Katrukha, “Analytical Issues with Natriuretic Peptides - has
611 this been Overly Simplified?,” *EJIFCC*, vol. 27, no. 3, pp. 189–207, Aug. 2016.

- 612 [12] P. A. Kavsak *et al.*, “Educational Recommendations on Selected Analytical and
613 Clinical Aspects of Natriuretic Peptides with a Focus on Heart Failure: A Report from
614 the IFCC Committee on Clinical Applications of Cardiac Bio-Markers,” *Clin Chem*,
615 vol. 65, no. 10, pp. 1221–1227, Oct. 2019, doi: 10.1373/clinchem.2019.306621.
- 616 [13] Y.-Y. Lee, B. Sriram, S.-F. Wang, S. Kogularasu, and G.-P. Chang-Chien, “Advanced
617 Nanomaterial-Based Biosensors for N-Terminal Pro-Brain Natriuretic Peptide
618 Biomarker Detection: Progress and Future Challenges in Cardiovascular Disease
619 Diagnostics,” *Nanomaterials*, vol. 14, no. 2, p. 153, Jan. 2024, doi:
620 10.3390/nano14020153.
- 621 [14] R. Maalouf and S. Bailey, “A review on B-type natriuretic peptide monitoring: assays
622 and biosensors,” *Heart Fail Rev*, vol. 21, no. 5, pp. 567–578, Sep. 2016, doi:
623 10.1007/s10741-016-9544-9.
- 624 [15] M. Gachpazan *et al.*, “A review of biosensors for the detection of B-type natriuretic
625 peptide as an important cardiovascular biomarker,” *Anal Bioanal Chem*, vol. 413, no.
626 24, pp. 5949–5967, Oct. 2021, doi: 10.1007/s00216-021-03490-6.
- 627 [16] H. Alawieh, T. El Chemaly, S. Alam, and M. Khraiche, “Towards Point-of-Care Heart
628 Failure Diagnostic Platforms: BNP and NT-proBNP Biosensors,” *Sensors*, vol. 19, no.
629 22, p. 5003, Nov. 2019, doi: 10.3390/s19225003.
- 630 [17] M. P. Sousa, P. Bettencourt, C. Brás-Silva, and C. Pereira, “Biosensors for natriuretic
631 peptides in cardiovascular diseases. A review,” *Curr Probl Cardiol*, vol. 49, no. 1, p.
632 102180, Jan. 2024, doi: 10.1016/j.cpcardiol.2023.102180.
- 633 [18] S. Ding, A. Cargill, S. Das, I. Medintz, and J. Claussen, “Biosensing with Förster
634 Resonance Energy Transfer Coupling between Fluorophores and Nanocarbon
635 Allotropes,” *Sensors*, vol. 15, no. 6, pp. 14766–14787, Jun. 2015, doi:
636 10.3390/s150614766.
- 637 [19] A. Tu *et al.*, “Detection of B-type natriuretic peptide by establishing a low-cost and
638 replicable fluorescence resonance energy transfer platform,” *Microchimica Acta*, vol.
639 187, no. 6, p. 331, Jun. 2020, doi: 10.1007/s00604-020-04247-1.
- 640 [20] X. Gong, J. Wu, J. Zhang, Z. Jiang, Y. Wang, and P. Zhang, “A Robust N-Terminal
641 Pro-Brain Natriuretic Peptide Assay for Clinical Diagnosis of Heart Failure in Elderly
642 Patients,” *J Anal Test*, vol. 8, no. 1, pp. 74–82, Mar. 2024, doi: 10.1007/s41664-023-
643 00270-2.
- 644 [21] M. K. Abraham *et al.*, “Luminescence ‘Turn-On’ Sensing of Brain Natriuretic Peptide
645 (BNP) - Dilated Cardiomyopathy Biomarker Based on the MoS₂ Nanosheet Quenched
646 Terbium Citrate Complex,” *ACS Appl Bio Mater*, vol. 7, no. 9, pp. 6044–6054, Sep.
647 2024, doi: 10.1021/acsabm.4c00676.
- 648 [22] X. Liu *et al.*, “Triple Cascade Quantum-Strip for Heart Failure Point-of-Care Testing,”
649 *ACS Sens*, vol. 9, no. 1, pp. 29–41, Jan. 2024, doi: 10.1021/acssensors.3c01217.
- 650 [23] Y. Gao *et al.*, “Near-infrared Persistent Luminescence Nanoparticles-Based
651 Immunochromatographic Assay for Autofluorescence-free Detection,” *ACS Appl Nano*
652 *Mater*, vol. 7, no. 17, pp. 20820–20828, Sep. 2024, doi: 10.1021/acsanm.4c03766.
- 653 [24] D. Strohmaier-Nguyen, C. Horn, and A. J. Baeumner, “NT-proBNP detection with a
654 one-step magnetic lateral flow channel assay,” *Anal Bioanal Chem*, vol. 416, no. 10,
655 pp. 2411–2422, Apr. 2024, doi: 10.1007/s00216-024-05223-x.
- 656 [25] H.-L. Liu, Y.-T. Tseng, M.-C. Lai, and L.-K. Chau, “Ultrasensitive and Rapid
657 Detection of N-Terminal Pro-B-Type Natriuretic Peptide (NT-proBNP) Using Fiber
658 Optic Nanogold-Linked Immunosorbent Assay,” *Biosensors (Basel)*, vol. 12, no. 9, p.
659 746, Sep. 2022, doi: 10.3390/bios12090746.

- 660 [26] D. Zheng *et al.*, “A Raman immunosensor based on SERS and microfluidic chip for
661 all-fiber detection of brain natriuretic peptide,” *Infrared Phys Technol*, vol. 125, p.
662 104252, Sep. 2022, doi: 10.1016/j.infrared.2022.104252.
- 663 [27] Y. Wang *et al.*, “A colorimetric and SERS-based LFIA for sensitive and simultaneous
664 detection of three stroke biomarkers: An ultra-fast and sensitive point-of-care testing
665 platform,” *Talanta*, vol. 283, p. 127166, Feb. 2025, doi:
666 10.1016/j.talanta.2024.127166.
- 667 [28] N. Chaturvedi, R. Arias, D. Tu, S. Mabbott, and G. L. Coté, “A low-cost, paper fluidic
668 platform to detect B-type Natriuretic Peptide (BNP) for Congestive Heart Failure
669 (CHF),” in *Optical Diagnostics and Sensing XXII: Toward Point-of-Care Diagnostics*,
670 G. L. Coté, Ed., SPIE, Mar. 2022, p. 8. doi: 10.1117/12.2607695.
- 671 [29] V. Quagliariello *et al.*, “Combinatorial immune checkpoint blockade increases
672 myocardial expression of NLRP-3 and secretion of H-FABP, NT-Pro-BNP,
673 interleukin-1 β and interleukin-6: biochemical implications in cardio-immuno-
674 oncology,” *Front Cardiovasc Med*, vol. 11, Jan. 2024, doi:
675 10.3389/fcvm.2024.1232269.
- 676 [30] Y. Wang *et al.*, “A colorimetric and SERS-based LFIA for sensitive and simultaneous
677 detection of three stroke biomarkers: An ultra-fast and sensitive point-of-care testing
678 platform,” *Talanta*, vol. 283, p. 127166, Feb. 2025, doi:
679 10.1016/j.talanta.2024.127166.
- 680 [31] H. Tan *et al.*, “An ultrasensitive nanozyme-based immunochromatographic platform
681 for quantitative detection of NT-proBNP using V2(Sn0.8Pt0.2)C MAX phase,” *Sens
682 Actuators B Chem*, vol. 418, p. 136223, Nov. 2024, doi: 10.1016/j.snb.2024.136223.
- 683 [32] Y.-Y. Chen, S.-L. Li, H.-L. Lin, W.-D. Li, X.-Z. Zhu, and H.-L. Zhang, “A
684 chemiluminescence immunoassay for the detection of NT-proBNP,” *Anal Biochem*,
685 vol. 611, p. 113950, Dec. 2020, doi: 10.1016/j.ab.2020.113950.
- 686 [33] F. Li, Q. Li, X. Shi, Y. Zhao, and Z. Guo, “Chemiluminescence immunoassay
687 amplified by functional acridinium ester for the detection of NT-proBNP in clinical
688 samples,” *Dyes and Pigments*, vol. 230, p. 112353, Nov. 2024, doi:
689 10.1016/j.dyepig.2024.112353.
- 690 [34] C.-S. Lau *et al.*, “Performance of the Abbott Architect Immuno-Chemiluminometric
691 NT-proBNP Assay,” *Diagnostics*, vol. 12, no. 5, p. 1172, May 2022, doi:
692 10.3390/diagnostics12051172.
- 693 [35] P. Feng *et al.*, “Analytical and clinical performance evaluation of a new NT-proBNP
694 assay,” *BMC Cardiovasc Disord*, vol. 24, no. 1, p. 341, Jul. 2024, doi:
695 10.1186/s12872-024-03994-w.
- 696 [36] H.-C. Li, X. He, S.-P. Qiao, Z.-N. Liu, and Y.-Z. Gao, “Development of an NT-
697 ProBNP Assay Reagent Based on High Specific Activity Alkaline Phosphatase CMAP
698 and an Improved Coupling Method,” *Applied Sciences*, vol. 10, no. 23, p. 8682, Dec.
699 2020, doi: 10.3390/app10238682.
- 700 [37] J. Cho, J.-H. Lee, and S.-G. Lee, “Evaluation of Analytical Performances and
701 Comparison of 3 NT-proBNP Assays for Diagnosing Heart Failure,” *Arch Pathol Lab
702 Med*, vol. 147, no. 8, pp. 949–956, Aug. 2023, doi: 10.5858/arpa.2021-0587-OA.
- 703 [38] J. Wen *et al.*, “Recent advances in zwitterionic polymers-based non-fouling coating
704 strategies for biomedical applications,” *Mater Today Chem*, vol. 40, p. 102232, Sep.
705 2024, doi: 10.1016/j.mtchem.2024.102232.
- 706 [39] S. Saxena, Y. Lu, Z. Zhang, Y. Li, L. Soleymani, and T. Hoare, “Zwitter-repel: An
707 anti-fouling coating promoting electrochemical biosensing in biological fluids,”
708 *Chemical Engineering Journal*, vol. 495, p. 153522, Sep. 2024, doi:
709 10.1016/j.cej.2024.153522.

- 710 [40] Q. Du, W. Wang, X. Zeng, and X. Luo, "Antifouling zwitterionic peptide hydrogel
711 based electrochemical biosensor for reliable detection of prostate specific antigen in
712 human serum," *Anal Chim Acta*, vol. 1239, p. 340674, Jan. 2023, doi:
713 10.1016/j.aca.2022.340674.
- 714 [41] C. Regev, Z. Jiang, R. Kasher, and Y. Miller, "Distinct Antifouling Mechanisms on
715 Different Chain Densities of Zwitterionic Polymers," *Molecules*, vol. 27, no. 21, p.
716 7394, Oct. 2022, doi: 10.3390/molecules27217394.
- 717 [42] K. Völlmecke *et al.*, "Hydrogel-Based Biosensors," *Gels*, vol. 8, no. 12, p. 768, Nov.
718 2022, doi: 10.3390/gels8120768.
- 719 [43] Y. Cui, Y. Zhang, L. Wang, and Y. Hao, "Recent Advances in Hydrogel-Promoted
720 Photoelectrochemical Sensors," *Biosensors (Basel)*, vol. 15, no. 8, p. 524, Aug. 2025,
721 doi: 10.3390/bios15080524.
- 722 [44] Y. Gu *et al.*, "Recent advances of MOF-based SERS substrates in quantitative analysis
723 of food contaminants: a review," *Analyst*, vol. 149, no. 20, pp. 4997–5013, 2024, doi:
724 10.1039/D4AN00897A.
- 725 [45] Roche Diagnostics, "Elecsys® proBNP II." Accessed: Sep. 09, 2025. [Online].
726 Available: [https://diagnostics.roche.com/global/en/products/lab/elecsys-probnp-ii-cps-
727 000499.html](https://diagnostics.roche.com/global/en/products/lab/elecsys-probnp-ii-cps-000499.html)
- 728 [46] C.-S. Lau *et al.*, "Performance of the Abbott Architect Immuno-Chemiluminometric
729 NT-proBNP Assay," *Diagnostics*, vol. 12, no. 5, p. 1172, May 2022, doi:
730 10.3390/diagnostics12051172.
- 731 [47] Siemens Healthineers, "Atellica Solution." Accessed: Sep. 09, 2025. [Online].
732 Available: [https://www.siemens-healthineers.com/laboratory-diagnostics/clinical-
733 chemistry-and-immunoassay-systems/atellica-solution-analyzers](https://www.siemens-healthineers.com/laboratory-diagnostics/clinical-chemistry-and-immunoassay-systems/atellica-solution-analyzers)
- 734 [48] Radiometer, "AQT90 FLEX immunoassay analyser." Accessed: Sep. 09, 2025.
735 [Online]. Available: [https://www.radiometer.ie/en-gb/products/immunoassay-
736 testing/aqt90-flex-immunoassay-analyser](https://www.radiometer.ie/en-gb/products/immunoassay-testing/aqt90-flex-immunoassay-analyser)
- 737 [49] Roche, "LumiraDx NT-proBNP." Accessed: Sep. 09, 2025. [Online]. Available:
738 [https://diagnostics.roche.com/global/en/products/lab/lumiradx-nt-probnp-
739 pid00000895.html](https://diagnostics.roche.com/global/en/products/lab/lumiradx-nt-probnp-pid00000895.html)
- 740 [50] K. Kant and S. Abalde-Cela, "Surface-Enhanced Raman Scattering Spectroscopy and
741 Microfluidics: Towards Ultrasensitive Label-Free Sensing," *Biosensors (Basel)*, vol. 8,
742 no. 3, p. 62, Jun. 2018, doi: 10.3390/bios8030062.
- 743 [51] Roche, "cobas® h 232 POC system." Accessed: Sep. 09, 2025. [Online]. Available:
744 [https://diagnostics.roche.com/global/en/products/instruments/cobas-h-232-ins-
745 653.html](https://diagnostics.roche.com/global/en/products/instruments/cobas-h-232-ins-653.html)
- 746 [52] Siemens, "Stratus® CS Acute Care™ Troponin Analyzer." Accessed: Sep. 09, 2025.
747 [Online]. Available: [https://www.siemens-healthineers.com/cardiac/cardiac-
748 systems/stratus-cs-acute-care](https://www.siemens-healthineers.com/cardiac/cardiac-systems/stratus-cs-acute-care)
- 749
750